Progress In Electromagnetics Research M, Vol. 115, 163–173, 2023

Angular Localization of Radio-Frequency Sources Using a Compact Metamaterial Receive Antenna

Abdelwaheb Ourir[1, *], Arnaud Tourin[1], Mathias Fink[1], Mohamed Kamoun[2], and Julien de Rosny[1]

Abstract—Radio-frequency source localization becomes a major challenge for many applications such as beam-steering or MIMO communication. This task is commonly carried out by taking advantage of the adjustable radiation patterns of phased arrays to scan an area. Nevertheless, it can be difficult and expensive to implement in some frequency bands of the last generation of communication systems. Here, we propose an alternative based on a single port compact metamaterial antenna. We use a finite periodic array of sub-wavelength ($\lambda/6$) resonators for the design of this antenna. A microstrip line is added to excite the resonator array etched on a grounded low-loss substrate and to use it as a planar antenna. In such an antenna system, the coupling between sub-wavelength resonators is able to induce a strong dispersion and leads to several complex radiation patterns over a specific narrow frequency band. We implement numerical methods to estimate the direction of a target antenna by taking benefits of the complex frequency signatures. We experimentally demonstrate that a single port sub-wavelength antenna made of a finite array of metamaterial resonators is able to retrieve the direction of a narrow band (3.6% relative bandwidth) emitting target around 5.5 GHz with a maximum precision of 3°. Such a compact planar system ($\lambda/3$, $\lambda/2$ and $2\lambda/3$) can be used to substitute the phased array localization technique in order to provide the necessary angular information in many applications such as mm-Wave communication and can be extended to high frequency regimes by using the corresponding resonators.

1. INTRODUCTION

Since the beginning of the 20th century, the localization of radio-sources is a major research domain for navigation, tracking, or monitoring services for military or civil purposes. Nowadays, for most of outdoor applications, localization is based on the time-of-flight measurements between a constellation of satellites and a receiving device (GPS, Galileo, GLONASS and Beidou). However, this solution is inoperative for indoor localization [1].

Indoor localization systems are principally based on a network of independent, decentralized antennas. These systems use the signal strength indicator as the basis for an approximate localization of an RF source [2].

For a better accuracy, one can use an antenna array and perform the beamforming of the signals received by each antenna. With the introduction of the fifth generation (5G) technology standard for cellular networks, these devices are now commonly used for massive MIMO (multiple-input-multiple-output) communications. Indeed MIMO antennas are also able to achieve, indoor and outdoor, high accuracy localization [3, 4]. For instance, massive MIMO has been employed to locate multiple users based on a fingerprinting localization in [5]. A massive MIMO-like system has also been proposed for

Received 17 October 2022, Accepted 22 January 2023, Scheduled 16 March 2023

* Corresponding author: Abdelwaheb Ourir (a.ourir@espci.fr).

[1] ESPCI Paris, Université PSL, CNRS, Paris 75005, France. [2] Mathematical and Algorithmic Science Lab, France Research Center, Huawei Technologies Co., Ltd., France.

simultaneous localization and mapping [3, 6]. Recently, MIMO mm-Wave localization in applications related to assisted living and location awareness has been considered in Ref. [7].

Angular localization is enough to reach the optimal system capacity in the majority of radio communication scenarios. For instance, this angular information is sufficient for a base station to focus energy toward a terminal in a line-of-sight scenario. Actually, this task can be achieved by MIMO antennas as explained previously. However, arrays imply that every antenna has its own RF chain [1, 8], and all of them are perfectly synchronized. Such MIMO systems have several disadvantages such as high cost, high-power consumption, and may require intensive computing algorithms [9]. Besides, the space limitation in the new generation communication systems makes the fulfillment of a high isolation between the radiators a tough challenge [10]. Various decoupling methods have been proposed and have shown the roughness of such task [11–14].

We have recently presented a metamaterial based antenna that is able to retrieve the angular position of a potential RF emitter [15]. The designed antenna achieves the desired angular localization thanks to the backfire-to-endfire radiation patterns using a dominant mode leaky-wave antenna proposed in Ref. [16]. Nevertheless, the proposed single port localizing system is only efficient when targeting wide band RF sources. Besides, the longitudinal dimension of the designed antenna is about two wavelengths and can be considered relatively bulky to be inserted in current mobile devices.

It has been shown in the last decades that sub-wavelength metamaterial resonators can intensely interact with the electric and magnetic fields [17–21]. These artificial electromagnetic structures have been proposed in various applications related to antenna systems in the last decades. For instance, it has been shown that specific properties of metallic composite material can modify the emission of an embedded source [22]. In particular, we have shown that metamaterials can generate a directive emission of electromagnetic sources [23]. Recently, metamaterials have been used for on-chip antennas applicable in THz integrated circuits [24] and for for microwave imaging systems to tumor detection [25].

In an array of periodic sub-wavelength resonators, the coupling between cells is able to induce a strong dispersion of surface waves around the main resonant frequency. We have recently shown that an array of coupled split ring resonators (SRRs) shows many resonances over a specific frequency band at which the structure efficiently emits far-field radiation [26, 27]. In particular, even if the array is small compared to the wavelength, the structure is able to radiate complex patterns such as dipolar and quadrupolar. We have used such metamaterial arrays to design a multi-band and multi-pattern smart antenna [28] and to perform sub-wavelength far field magnetic imaging [29, 30]. Here, we propose to take benefits of the complex radiation patterns of metamaterial arrays in order to achieve the angular localization of electromagnetic emitters. The idea is to reduce the consuming task of localization, usually performed by phased arrays, to a straightforward narrow band frequency analysis of a signal received by a single compact antenna.

2. DESIGN OF UNIT CELL

The geometry of one unit cell that composes our metasurface shown in Fig. 1(a) is chosen because of its compactness. It is referred as an electric-LC (ELC) resonator and has been first introduced in [31]. Such metamaterial resonators, also called 2LC or L2C resonators, are suitable for implementing high impedance walls or specific media with desired positive or negative permittivity in one to three dimensions [31, 32]. Because of its geometry, it can be modeled as 2 inductors (L) and one capacitor (C) in parallel (see Fig. 1(b)).

The ELC resonator is simulated using a full-wave commercial software (CST Studio). The resonator is on the top of a 1.6 mm-thick grounded Duroid substrate and is designed to show a fundamental resonant frequency around 5.2 GHz. The band structure of a periodic surface made of ELC resonators is shown in Fig. 1(c). It is calculated for the transverse electric (TE) configuration where the electric field is parallel to the resonator. The lowest frequency band linked to the fundamental mode of the unit-cell lies between 4.9 GHz and 5.4 GHz. Within this frequency range, the lateral size of one unit cell is about a sixth of the free space wavelength. The surface current distribution of the fundamental mode of the unit cell shown in Fig. 1(d) confirms that this last mainly acts as an electrical dipole because the 2 magnetic dipoles are in opposite directions and cancel each other.

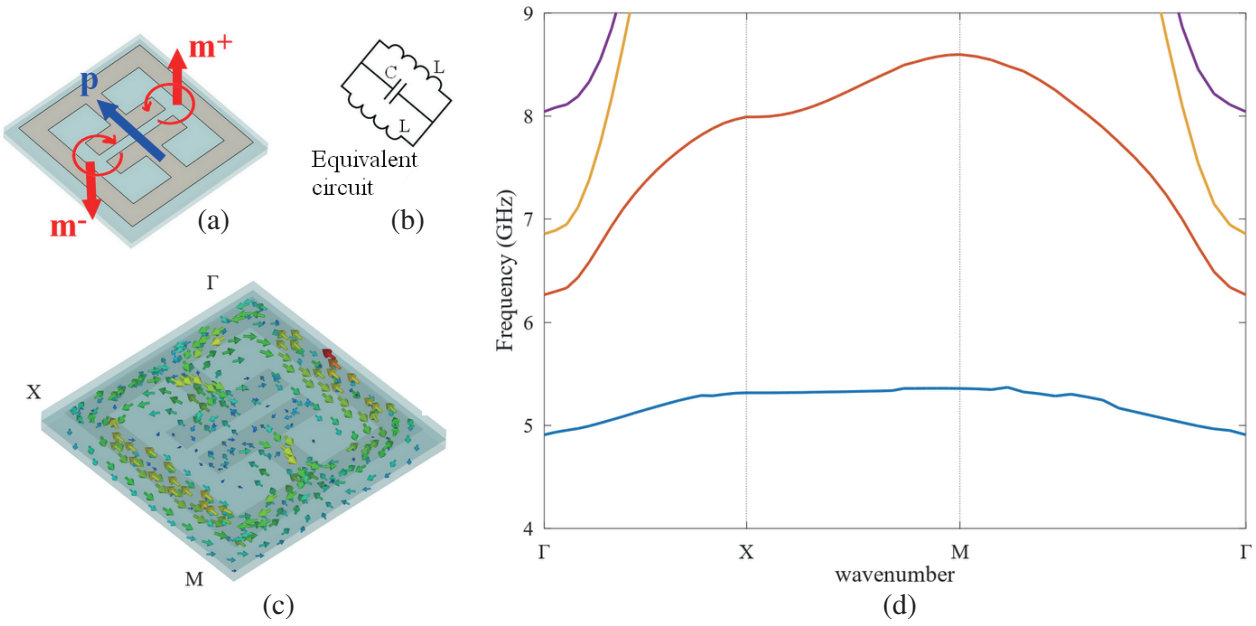

Figure 1. (a) ELC unit-cell geometry with electric and magnetic moments. (b) Equivalent circuit of the unit cell. (c) Simulated current distribution. (d) Band structure.

3. FINITE PERIODIC ARRAY

In order to obtain a unique angular and frequency signature on the radiated field over a specific frequency band, we propose to design a planar antenna based on a finite periodic array of ELC resonators. Fig. 2(a) shows the schematic view of the designed planar antenna. The resonators are arranged in a square lattice with a 9 mm period. To excite the proposed metamaterial array and use it as a planar antenna, we have etched a 50-Ohm microstrip line placed at 0.8 mm height of the dielectric substrate.

This microstrip line ends below the first cell placed at the array corner in order to excite the maximum modes of the structure through an electromagnetic coupling mechanism. This feeding system has been optimized in the simulation calculation and in the experimental designs to obtain the best return losses. As predicted (e.g., [26]) for such a finite array of metamaterial resonators, we obtain a set of discrete modes. Each mode is characterized by its resonance angular frequency ω_n and its dumping factor ζ_n. As a consequence, the electric field radiated at position ρ can be expressed as a superposition of the radiation by each mode

$$\mathbf{E}(\rho) = \sum_q a_q \frac{\sum_i p_i^q \overleftrightarrow{\mathbf{G}}(\rho, \mathbf{r}_i; \omega_n)\hat{\mathbf{x}}}{\omega^2 - j\zeta_n \omega \omega_q + \omega_q^2} \tag{1}$$

where p_i^q corresponds to the modal amplitude on the i-th resonator (at position $\mathbf{r}_i$) of the q-th mode. The complex number a_q depicts the coupling coefficient between the feed and the array of resonators. The 3 by 3 matrix $\overleftrightarrow{\mathbf{G}}$ is the far field dyadic Green's function that is given by

$$\overleftrightarrow{\mathbf{G}}(\rho, \mathbf{r}_i; \omega_n)\hat{\mathbf{x}} = \frac{k_n^2}{\epsilon_0}\hat{\rho} \times (\hat{\mathbf{x}} \times \hat{\rho}) \frac{e^{-jk_0\|\rho - \mathbf{r}_i\|}}{4\pi \|\rho - \mathbf{r}_i\|}, \tag{2}$$

where $k_n = \omega_n / c_0$ and $\hat{\rho} = \rho \| \rho \|$.

Because the term $\sum_i p_i^q \overleftrightarrow{\mathbf{G}}(\rho, \mathbf{r}_i; \omega_n)\hat{\mathbf{x}}$ is different for different probing directions, i.e., $\hat{\rho}$, the frequency signature of $\mathbf{E}$ also depends on this direction.

To quantitatively assess the diversity, full-wave simulations are performed using the time-domain solver of a commercial software (CST Studio). Fig. 2(b) shows the obtained reflection coefficient for

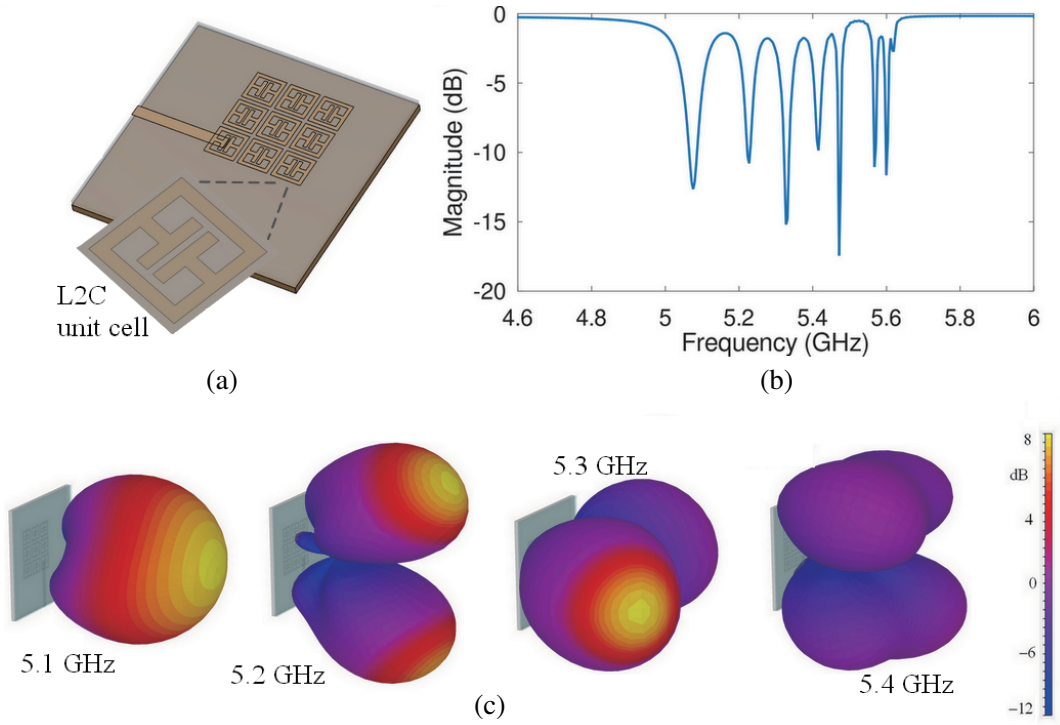

Figure 2. (a) Schematic view of the single port metamaterial antenna. The inset presents the L2C resonator unit cell. (b) The calculated reflection coefficient of the antenna. (c) Three-dimensional radiation patterns of the antenna calculated at the first 4 resonant frequencies.

the designed 3 by 3 finite array of metamaterial resonator based antenna. One can see a cluster of resonant frequencies between 5.1 and 5.6 GHz that corresponds to the first radiation frequency band of the structure. The radiation patterns of this metamaterial antenna calculated at the different resonant frequencies are plotted in Fig. 2(c). As predicted by Ref. [26] for such a finite array of metamaterial resonators, we obtain a notable radiation pattern diversity over the working band. We observe especially some expected complex radiation patterns such as dipolar and quadrupolar patterns. Finally, it is interesting to notice that the highest maximum gain of 4 dB is obtained for the first mode, while the lowest maximum gain of about −2 dB is observed on the highest mode radiation patterns.

4. EXPERIMENTAL CHARACTERIZATION

For the experimental demonstration in the microwave regime, we propose to consider 3 different finite arrays for the realization of the metamaterial antenna. The first antenna is a 2 by 2 periodic square array; the second is a 3 by 3 array; and the last antenna is made by a 4 by 4 periodic array. An Agilent Vector Network Analyzer (VNA) is used to measure the reflection coefficients. Fig. 3 shows these 3 different antennas and their measured reflection coefficient spectra, respectively. Despite the higher level of loss and the slight frequency shift observed in the experiment, a cluster of resonances is obtained in the 3 configurations as expected. One can also notice the increase of the number of resonances for the antenna made with a higher number of resonators. Actually, the number of modes is at maximum equal to the number of resonators [26].

We measure, with the VNA, the radiated field of the designed metamaterial antennas with respect to the frequency using the setup shown on Fig. 4(a). We use 3 different antenna receivers to collect the radiated signals. The first antenna is a WR-159 waveguide horn antenna showing a maximum gain of 15.4 dBi (at 6 GHz). A wide-band Vivaldi antenna of a mean average gain of 7 dBi is the second antenna receiver. The last antenna is a dipole antenna showing a maximum gain of 1.6 dBi. A comparison of the

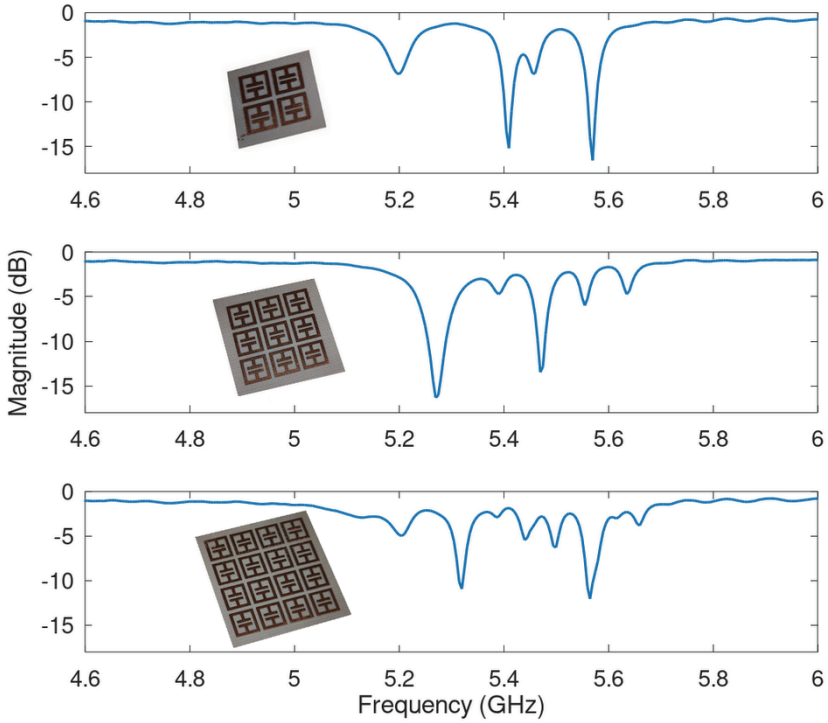

Figure 3. The measured reflection coefficients of the considered single port metamaterial antennas. Insets show pictures of the considered metamaterial arrays used for the realization of the antennas.

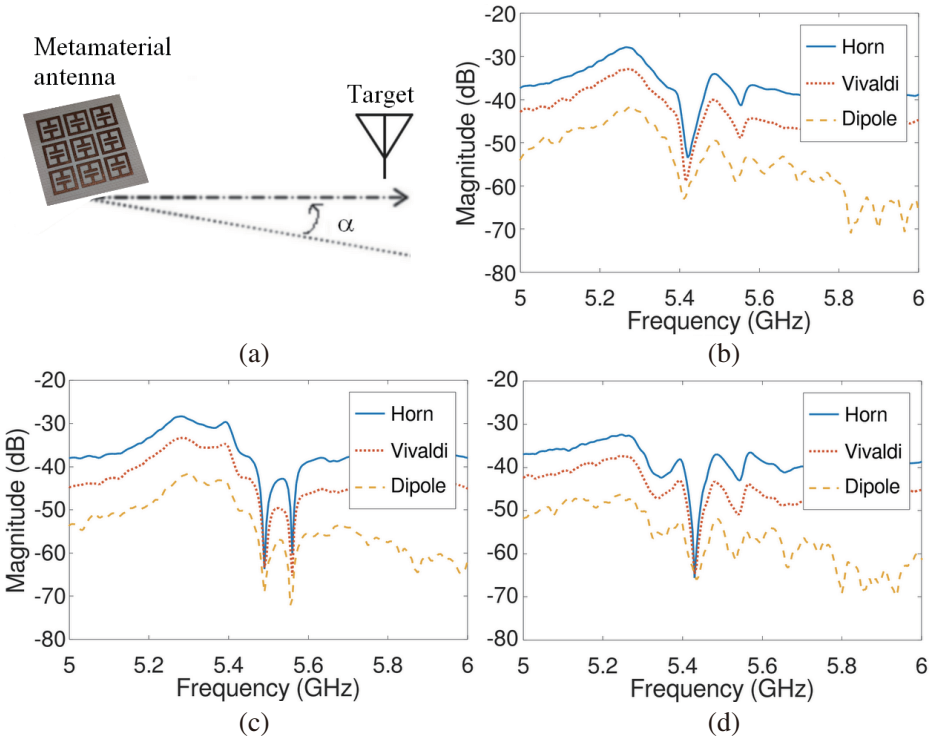

Figure 4. (a) Schematic view of the angular localization scenario using a single port metamaterial antenna receiver. The radiated spectra measured by the 3 by 3 metamaterial antenna for 3 different antennas respectively at $-45°$ (b), $0°$ (c) and $45°$ (d).

spectra obtained with these antennas for 3 different angles of radiation is presented in Fig. 4. One can notice the effect of the gain on the level of the measured signals. In particular, a high level of noise is observed on the signal collected with the dipole receiver leading to a poor signal-to-noise ratio (SNR). We can also notice the unique spectrum signature received by the metamaterial antenna for each angle.

5. ANGULAR LOCALIZATION OF RADIO-FREQUENCY SOURCES

The angular localization we propose is based on the angular and frequency diversities of the metamaterial radiating structures. Thanks to the unique spectrum in the working band radiated at each angle, we aim to recognize the direction of the radiation emitted by an antenna placed at the far field of the metamaterial structure. We use the radiation pattern $S_0(\theta, \nu)$ (modulus of the S_{12} parameter) measured between the metamaterial antenna and the waveguide horn antenna as the reference patterns where θ is the angles between the axes of the two antennas, and ν is the frequency. This collection of radiation patterns is called dictionary.

In order to find the most similar element of the dictionary and therefore the direction of the emitting antenna, we compute the normalized correlation coefficients between the dictionary elements and the response of the antenna of unknown direction. To that end we introduce the normalized dictionary matrix. One element $(\hat{S}_0)_{i,j}$ of this matrix is the S-parameter for an incident angle θ_j and a frequency ν_i. The normalization is such that $\sum_i (\hat{S}_0)^2_{i,j} = 1$. The result of the correlation is a vector $\mathbf{C}$ given by

$$\mathbf{C} = \hat{\mathbf{S}}_0^T \mathbf{S}_t, \tag{3}$$

where $\mathbf{S}_t$ is the frequency response of the antenna of unknown direction. The index of the maximum of $\mathbf{C}$ is associated with the most probable incidence angle. Correlation based methods are known to be robust to the presence of noise.

To test the independence of the method to find the direction of other antennas, the Vivaldi and dipole antennas have been tested with the dictionary constructed with the measurements obtained with the waveguide horn antenna. For each antenna, 180 incident angles have been tested (between $-90°$ and $90°$ with a step of $5°$). A frequency band of 500 MHz with a 5 MHz frequency step is used for the correlation procedure. The considered frequency band is between 5.15 and 5.65 GHz which corresponds to 9% of relative frequency band.

The first 6 plots of Fig. 5 show the results obtained for the Vivaldi and dipole emitter antennas by considering the 500 MHz frequency bandwidth. The plots of Fig. 5, from top to bottom, correspond to the results from the 2 by 2 to the 4-by-4-metamaterial antenna receivers for E-plane radiation. We first notice that the incident angle of the Vivaldi antenna is globally recovered with the 3 considered metamaterial configurations. Furthermore, an enhancement of the precision is observed by increasing the number of resonators in the metamaterial array, especially for the large angles. The best 5% precision is observed for all the angles with the largest metamaterial receiver made by an array of 4 by 4 sub-wavelength resonators. This result can be explained by the highest radiation diversity generated by the largest metamaterial array. In such a case, the data carefully fit the dictionary elements. This is not the case for the dipole antenna for all the 3 configurations. Because of the low gain, the correlation algorithm fails to recover the incident angles, especially the large ones. This is due to the bad signal to noise ratio that induces some fluctuations on the measured signals. Nevertheless, the enhancement of the precision by increasing the number of resonators in the metamaterial array is still observable in this configuration. A precision of 5% is attained thereby for angles between $-60°$ and $60°$ by using the largest metamaterial array.

In the transition to the new generations of communication systems, 5G and shortly 6G, broad bandwidths are expected at higher frequencies in order to increase the data rates. Nevertheless, the future communication systems will be a combination of sub-6 GHz, mm-wave bands and THz bands operating with a diversity of relative frequency bandwidths. While the 9% of a relative frequency band used here for our localization procedure can be considered realistic for some communication systems, and smaller relative frequency bandwidths could be appropriate in other scenarios.

Thereafter, we propose to experiment our procedure of localization using a smaller frequency bandwidth. The implemented correlation algorithm is then limited to a frequency band of 200 MHz which corresponds to a relative frequency band of 3.6% at 5.5 GHz. Moreover, in order to take benefits

of the maximum of complex radiation patterns of the highest efficient modes, we perform the localization analysis process between 5.4 and 5.6 GHz for all the configurations.

The last 6 plots of Fig. 5 present the E-plane results obtained for the Vivaldi and dipole emitter targets by using a 200 MHz frequency bandwidth for the detection process. One can notice clearly a global loss on the detection precision for all the experimented configurations due to the bandwidth decrease. Nevertheless, for the Vivaldi target (plots at the left), the localization process still provides exploitable results with the 3 by 3 metamaterial array and even good results when using the metamaterial antenna receiver made by the largest array of 4 by 4 resonators. However, for the dipole antenna emitter (plots at the right), the localization algorithm fails to recover the dipole position for the largest part of the angles when the metamaterial antenna receiver is 2 by 2 or 3 by 3 resonator arrays. The fluctuations induced by the low received signal level substantially reduces the probability to recover the target in these configurations. Nevertheless, a slight enhancement of the results is observed when the largest metamaterial array is used.

The results presented in Fig. 5 are obtained in the E-plane configuration. Similar results and conclusions are observed for the H-plane measurements. A summary of all the achieved detection performances in E-plane is given in Table 1. It shows the standard deviation between the incident angle and the estimated one. We notice that when a narrow frequency band is considered, the proposed correlation based method fails to provide a good estimation of the target direction in the case of the dipole emitter. For this reason we test a second algorithm based on spectral equalization. To that end, first we perform the singular decomposition of the dictionary matrix, i.e.,

$$\hat{\mathbf{S}}_0 = \mathbf{USV}^H. \tag{4}$$

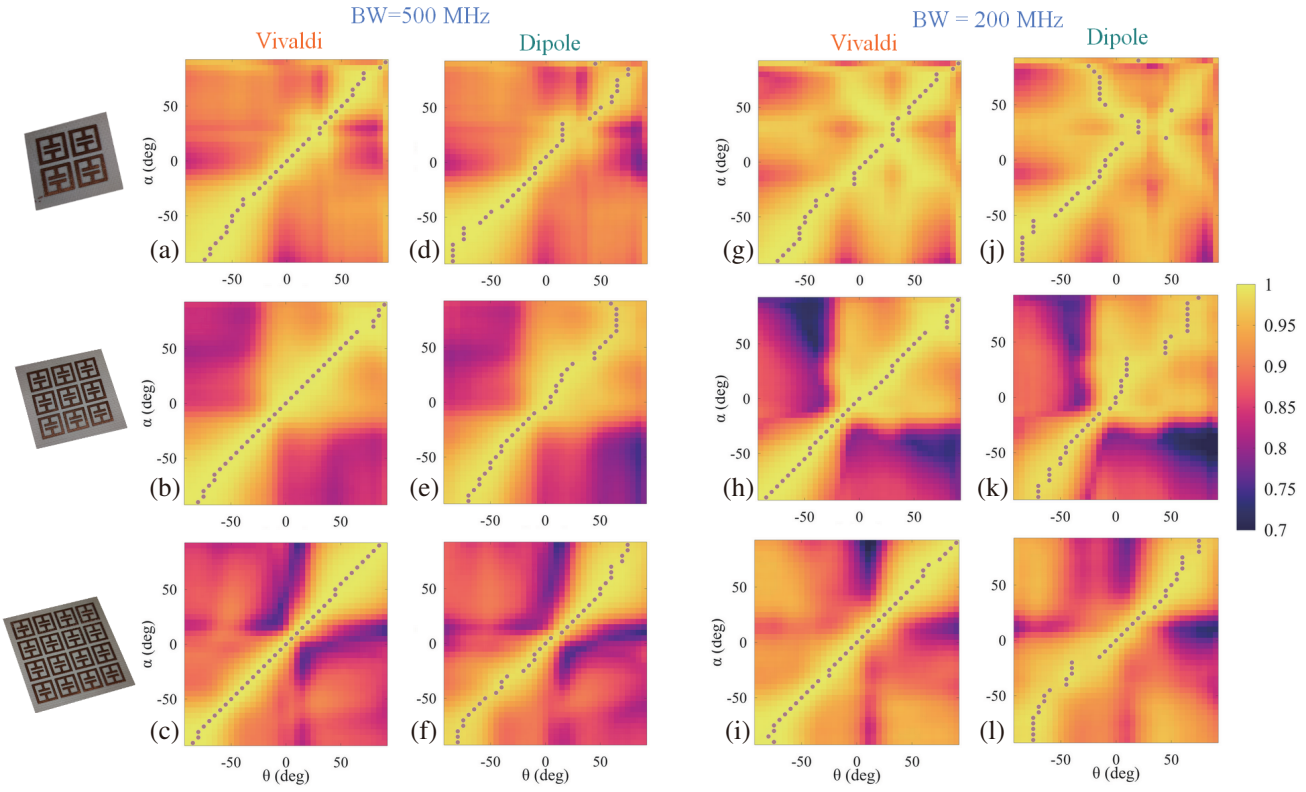

Figure 5. Detection angle maps calculated by the correlation algorithm using 500 MHz and 200 MHz frequency bandwidth. The vertical axis corresponds to the real angle of incidence (α) and the horizontal axis to tested angle (θ). The magenta dots show the maximum value (most likely angle). The color maps (a), (b), (c), (g), (h) and (i) are obtained for the Vivaldi antenna by using different dimension sizes of the metamaterial antenna receiver. Maps (d), (e), (f), (j), (k) and (l) are for the dipole antenna with the 3 different receivers.

Table 1. Standard deviations of the detected angles for the 3 different antennas and for the 2-detection processing.

2×2 metamaterial array	Vivaldi	Dipole
500 MHz	5.5°	10.1°
200 MHz	7.9°	42°
3×3 metamaterial array		
500 MHz	3.4°	9.7°
200 MHz	4.4°	10.2°
4×4 metamaterial array		
500 MHz	2.7°	5.6°
200 MHz	3°	8.5°

We then construct an equalized matrix such as

$$\hat{\mathbf{S}}_{eq} = \mathbf{U}\mathbf{V}^{H}. \tag{5}$$

The matching vector is then given as for the correlation by $\hat{\mathbf{S}}_{eq}^{T}\mathbf{S}_{t}$.

Figures 6(a) and (b) present the results obtained for the estimated direction of the dipole emitter using the singular value decomposition (SVD) equalization algorithm using respectively the 3 by 3 and 4 by 4 metamaterial antennas. The dictionary elements are limited to a frequency band lying between 5.4 and 5.6 GHz measured by the metamaterial receivers. One can notice that globally the maximum error on the prediction of the detected angles is reduced by using the SVD equalization algorithm. In the case of the 3 by 3 metamaterial antenna, the standard deviation of the detected angle is reduced to 10.2°. The SVD algorithm achieves even a 5.9° of standard deviation for the 4-by-4-metamaterial antenna. Generally, better performances can be obtained by considering enhanced algorithms for the target detection.

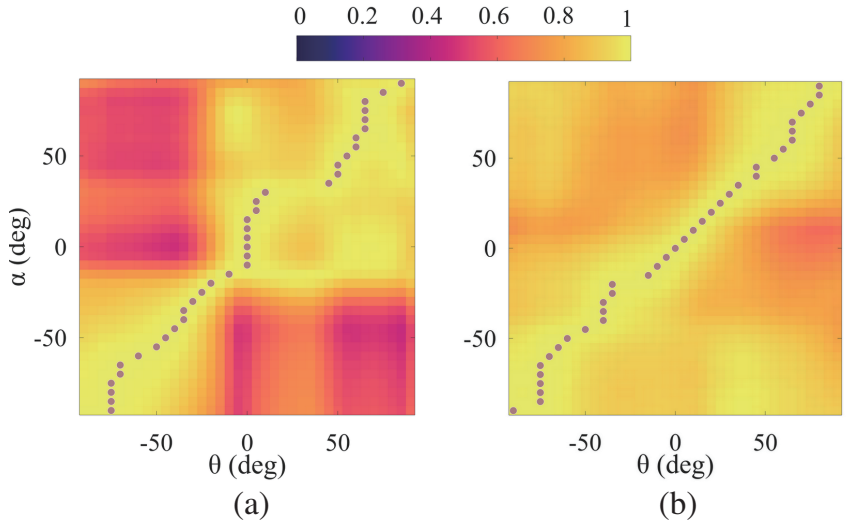

Figure 6. Detection angle maps calculated by the SVD algorithm using a 200 MHz frequency bandwidth for the dipole emitters using the 3 by 3 (a) and the 4 by 4 (b) metamaterial antenna receivers.

6. CONCLUSION

We have designed compact ($\lambda/3$, $\lambda/2$ and $2\lambda/3$) planar antennas that are able to achieve complex radiation patterns over a narrow frequency band. Finite periodic arrays of sub-wavelength ($\lambda/6$) metamaterial resonators have been used for the realization of these antennas. The full-wave simulation and experimental characterization have shown that the antennas are able to generate unique angular signatures at far field over the working frequency band. We have experimentally demonstrated that such antennas can be used to retrieve the angular position of a potential emitter by taking benefits of the achieved angular signatures. By using these single port sub-wavelength antennas, we have determined the direction of a narrow band (3.6% relative bandwidth) emitting target around 5.5 GHz with a maximum precision of 3°. This approach, based on a single port metamaterial antenna, can be used to substitute the phased array localization technique and to provide an important angular information about RF radiating sources. For instance, it can be used to focus energy in many applications such as mm-Wave communication. The proposed localization technique can be extended to high frequency regimes by using resonators dedicated to such bands.

ACKNOWLEDGMENT

This work has received support under the program "Investissements d'Avenir" launched by the French Government.

REFERENCES

1. Chia, M. Y. W., L. Brás, N. B. Carvalho, Pinho, L. Kulas, and K. Nyka, "A review of antennas for indoor positioning systems," *International Journal of Antennas and Propagation*, Vol. 2012, 953269, 2012.
2. Cheng, C.-H. and Y. Yan, "Indoor positioning system for wireless sensor networks based on two-stage fuzzy inference," *International Journal of Distributed Sensor Networks*, Vol. 14, 1550147718780649, May 2018.
3. Garcia, N., H. Wymeersch, E. G. Larsson, A. M. Haimovich, and M. Coulon, "Direct localization for massive MIMO," *IEEE Transactions on Signal Processing*, Vol. 65, No. 10, 2475–2487, 2017.
4. Guerra, A., F. Guidi, and D. Dardari, "Position and orientation error bound for wideband massive antenna arrays," *2015 IEEE International Conference on Communication Workshop (ICCW)*, 853–858, 2015.
5. Savic, V. and E. G. Larsson, "Fingerprinting-based positioning in distributed massive MIMO systems," *2015 IEEE 82nd Vehicular Technology Conference (VTC2015-Fall)*, 1–5, 2015.
6. Guidi, F., A. Guerra, and D. Dardari, "Personal mobile radars with millimeter-wave massive arrays for indoor mapping," *IEEE Transactions on Mobile Computing*, Vol. 15, No. 6, 1471–1484, 2016.
7. Witrisal, K., Meissner, E. Leitinger, Y. Shen, C. Gustafson, F. Tufvesson, K. Haneda, D. Dardari, A. F. Molisch, A. Conti, and M. Z. Win, "High-accuracy localization for assisted living: 5G systems will turn multipath channels from foe to friend," *IEEE Signal Processing Magazine*, Vol. 33, No. 2, 59–70, 2016.
8. Qiu, L., X. Liang, and Z. Huang, "Patl: A RFID tag localization based on phased array antenna," *Scientific Reports*, Vol. 7, No. 1, 44183, 2017.
9. Du, H., C. Zhang, Q. Ye, W. Xu, L. Kibenge, and K. Yao, "A hybrid outdoor localization scheme with high-position accuracy and low-power consumption," *EURASIP Journal on Wireless Communications and Networking*, Vol. 2018, No. 1, 4, 2018.
10. Alibakhshikenari, M., F. Babaeian, B. S. Virdee, S. Aïssa, L. Azpilicueta, C. H. See, A. A. Althuwayb, I. Huynen, R. A. Abd-Alhameed, F. Falcone, and E. Limiti, "A comprehensive survey on 'various decoupling mechanisms with focus on metamaterial and metasurface principles applicable to SAR and MIMO antenna systems'," *IEEE Access*, Vol. 8, 192965–193004, 2020.

11. Alibakhshikenari, M., B. S. Virdee, H. Benetatos, E. M. Ali, M. Soruri, M. Dalarsson, M. Naser-Moghadasi, C. H. See, A. Pietrenko-Dabrowska, S. Koziel, S. Szczepanski, and E. Limiti, "An innovative antenna array with high inter element isolation for sub-6 GHz 5G MIMO communication systems," *Scientific Reports*, Vol. 12, No. 1, 7907, 2022.
12. Alibakhshikenari, M., B. S. Virdee, Shukla, C. H. See, R. A. Abd-Alhameed, F. Falcone, K. Quazzane, and E. Limiti, "Isolation enhancement of densely packed array antennas with periodic MTM-photonic bandgap for SAR and MIMO systems," *IET Microwaves, Antennas & Propagation*, Vol. 14, No. 3, 183–188, 2020.
13. Alibakhshikenari, M., B. S. Virdee, C. H. See, R. A. Abd-Alhameed, F. Falcone, and E. Limiti, "Surface wave reduction in antenna arrays using metasurface inclusion for MIMO and SAR systems," *Radio Science*, Vol. 54, No. 11, 1067–1075, 2019.
14. Alibakhshikenari, M., B. S. Virdee, Shukla, C. H. See, R. Abd-Alhameed, M. Khalily, F. Falcone, and E. Limiti, "Antenna mutual coupling suppression over wideband using embedded periphery slot for antenna arrays," *Electronics*, Vol. 7, No. 9, 2018.
15. Ourir, A., A. Mokh, R. Khayatzadeh, M. Kamoun, A. Tourin, A. Fink, and J. de Rosny, "Angular localization of wideband sources using a single port metamaterial receive antenna," *2022 16th European Conference on Antennas and Propagation (EuCAP)*, 1–4, 2022.
16. Liu, L., C. Caloz, and T. Itoh, "Dominant mode leaky-wave antenna with backfire-to-endfire scanning capability," *Electronics Letters*, Vol. 38, No. 2, 1414–1416, Nov. 2002.
17. Pendry, J. B., A. J. Holden, W. J. Stewart, and I. Youngs, "Extremely low frequency plasmons in metallic mesostructures," *Phys. Rev. Lett.*, Vol. 76, 4773–4776, Jun. 1996.
18. Pendry, J., A. Holden, D. Robbins, and W. Stewart, "Magnetism from conductors and enhanced nonlinear phenomena," *IEEE Transactions on Microwave Theory and Techniques*, Vol. 47, 2075–2084, Nov. 1999.
19. Abdeddaim, R., A. Ourir, and J. de Rosny, "Realizing a negative index metamaterial by controlling hybridization of trapped modes," *Phys. Rev. B*, Vol. 83, 033101, Jan. 2011.
20. Ourir, A., R. Abdeddaim, and J. de Rosny, "Double-T metamaterial for parallel and normal transverse electric incident waves," *Opt. Lett.*, Vol. 36, 1527–1529, May 2011.
21. Ourir, A. and H. H. Ouslimani, "Negative refractive index in symmetric cut-wire pair metamaterial," *Applied Physics Letters*, Vol. 98, No. 11, 113505, 2011.
22. Enoch, S., G. Tayeb, Sabouroux, N. Guérin, and Vincent, "A metamaterial for directive emission," *Phys. Rev. Lett.*, Vol. 89, 213902, Nov. 2002.
23. Ourir, A., A. de Lustrac, and J.-M. Lourtioz, "All-metamaterial-based subwavelength cavities (lambda/60) for ultrathin directive antennas," *Applied Physics Letters*, Vol. 88, No. 8, 084103, 2006.
24. Alibakhshikenari, M., E. M. Ali, M. Soruri, M. Dalarsson, M. Naser-Moghadasi, B. S. Virdee, C. Stefanovic, A. Pietrenko-Dabrowska, S. Koziel, S. Szczepanski, and E. Limiti, "A comprehensive survey on antennas on-chip based on metamaterial, metasurface, and substrate integrated waveguide principles for millimeter-waves and terahertz integrated circuits and systems," *IEEE Access*, Vol. 10, 3668–3692, 2022.
25. Alibakhshikenari, M., B. S. Virdee, Shukla, N. O. Parchin, L. Azpilicueta, C. H. See, R. A. Abd-Alhameed, F. Falcone, I. Huynen, T. A. Denidni, and E. Limiti, "Metamaterial-inspired antenna array for application in microwave breast imaging systems for tumor detection," *IEEE Access*, Vol. 8, 174667–174678, 2020.
26. Jouveaud, C., A. Ourir, and J. Rosny, "Surface waves radiation by finite arrays of magnetoelectric resonators," *Progress In Electromagnetics Research*, Vol. 132, 177–198, 2012.
27. Jouvaud, C., J. de Rosny, and A. Ourir, "Adaptive metamaterial antenna using coupled tunable split-ring resonators," *Electronics Letters*, Vol. 49, 518–519, Apr. 2013.
28. Jouvaud, C., A. Ourir, and J. Rosny, "Smart tuning," *Electronics Letters*, Vol. 49, No. 8, 512–512, 2013.

29. Ourir, A., G. Lerosey, F. Lemoult, M. Fink, and J. de Rosny, "Far field subwavelength imaging of magnetic patterns," *Applied Physics Letters*, Vol. 101, No. 11, 111102, 2012.
30. Jouvaud, C., A. Ourir, and J. de Rosny, "Far-field imaging with a multi-frequency metalens," *Applied Physics Letters*, Vol. 104, No. 24, 2014.
31. Schurig, D., J. J. Mock, and D. R. Smith, "Electric-field-coupled resonators for negative permittivity metamaterials," *Applied Physics Letters*, Vol. 88, No. 4, 041109, 2006.
32. Zhou, L., H. Ouslimani, A. Priou, A. Ourir, and O. Maas, "Understanding the behavior of miniaturized metamaterial-based dipole antennas in leaky wave regime," *Applied Physics A*, Vol. 106, No. 1, 145–149, 2012.